

# Phase transitions in two-dimensional anisotropic quantum magnets

Alessandro Cuccoli<sup>1</sup>, Tommaso Roscilde<sup>2</sup>, Valerio Tognetti<sup>1</sup>, Ruggero Vaia<sup>3</sup>, and Paola Verrucchi<sup>1</sup>

<sup>1</sup> Dipartimento di Fisica dell'Università di Firenze and Istituto Nazionale di Fisica della Materia (INFN), Largo E. Fermi 2, I-50125 Firenze, Italy

<sup>2</sup> Dipartimento di Fisica "A. Volta" dell'Università di Pavia and Istituto Nazionale di Fisica della Materia (INFN), via Bassi 6, I-27100 Pavia, Italy

<sup>3</sup> Istituto di Elettronica Quantistica del Consiglio Nazionale delle Ricerche, via Panciatichi 56/30, I-50127 Firenze, Italy, and Istituto Nazionale di Fisica della Materia (INFN)

October 31, 2018

**Abstract.** We consider quantum Heisenberg ferro- and antiferromagnets on the square lattice with exchange anisotropy of easy-plane or easy-axis type. The thermodynamics and the critical behaviour of the models are studied by the pure-quantum self-consistent harmonic approximation, in order to evaluate the spin and anisotropy dependence of the critical temperatures. Results for thermodynamic quantities are reported and comparison with experimental and numerical simulation data is made. The obtained results allow us to draw a general picture of the subject and, in particular, to estimate the value of the critical temperature for any model belonging to the considered class.

**PACS.** 75.10.Jm Quantized spin models – 75.10.-b General theory and models of magnetic ordering – 75.40.Cx Static properties

## 1 Introduction

In this paper we examine the class of magnetic models described by the Hamiltonian

$$\hat{\mathcal{H}} = -J \sum_{\langle \mathbf{i}\mathbf{j} \rangle} \left[ \mu \left( \hat{S}_{\mathbf{i}}^x \hat{S}_{\mathbf{j}}^x + \hat{S}_{\mathbf{i}}^y \hat{S}_{\mathbf{j}}^y \right) + \lambda \hat{S}_{\mathbf{i}}^z \hat{S}_{\mathbf{j}}^z \right] \quad (1)$$

where  $\mathbf{i} \equiv (i_1, i_2)$ ,  $\mathbf{j} \equiv (j_1, j_2)$  are sites on a square lattice, and the sum runs over the pairs of nearest neighbours; the spin degrees of freedom are described by the quantum operators  $\hat{\mathbf{S}}_{\mathbf{i}} \equiv (\hat{S}_{\mathbf{i}}^x, \hat{S}_{\mathbf{i}}^y, \hat{S}_{\mathbf{i}}^z)$ , obeying the angular momentum commutation relations  $[\hat{S}_{\mathbf{i}}^\alpha, \hat{S}_{\mathbf{j}}^\beta] = \epsilon^{\alpha\beta\gamma} \delta_{\mathbf{i}\mathbf{j}} \hat{S}_{\mathbf{i}}^\gamma$  with  $|\hat{\mathbf{S}}|^2 = S(S+1)$ .

For positive  $\lambda$  and  $\mu$ , the sign of the exchange integral  $J$  sets the ferro- or antiferromagnetic character of the model,  $J > 0$  or  $J < 0$  respectively; for the sake of a more compact notation, however, we will hereafter take a positive  $J$  and properly change the sign of  $\mu$  and  $\lambda$  to obtain the required antiferromagnetic Hamiltonian.

At a classical level, i.e. when  $S \rightarrow \infty$ , ferro- and antiferromagnets have the same static properties and can be simultaneously studied as far as their thermodynamics is concerned. On the other hand, when quantum fluctuations are taken into account, the two types of models display substantially different features. It is worthwhile noticing that, despite displaying the most interesting quantum fea-

tures, antiferromagnetic models are less affected by quantum fluctuations than ferromagnetic ones, as quantum renormalizations are sensibly stronger in the latter, whatever the approach used to evaluate them.

In this paper, the anisotropy parameters  $\mu$  and  $\lambda$  are set to range in the interval  $[-1, 1]$ , and the following sub-classes of models are hence considered:

(i) Isotropic:  $\mu = \lambda$ ,  $|\lambda| = 1$ , ferro- and antiferromagnetic ( $\lambda > 0$  and  $\lambda < 0$ , respectively).

(ii) Easy-plane:  $\mu = 1$ ,  $\lambda \in (-1, 1)$ , ferro- and antiferromagnetic ( $\lambda > 0$  and  $\lambda < 0$ , respectively).

(iii) Easy-axis:  $\mu \in (-1, 1)$ ,  $\lambda = \text{sign}(\mu)$ , ferro- and antiferromagnetic ( $\mu > 0$  and  $\mu < 0$ , respectively).

Models belonging to these sub-classes have the common feature of displaying, as the temperature decreases, a phase-transition towards a more ordered phase; this transition generically occurs at a critical temperature which is a function of both the spin value and the anisotropy parameters, and will be hereafter indicated by  $t_c(\nu, S)$ , with  $\nu = \mu, \lambda$  depending on the specific class considered, and the reduced temperature  $t$  defined by  $t \equiv T/J\tilde{S}^2$  with  $\tilde{S} \equiv S + 1/2$ .

(i) The isotropic model, both ferro- and antiferromagnetic, has the full rotational  $O(3)$  symmetry and it is hence in a paramagnetic phase down to  $t = 0$ , as required by the Mermin-Wagner theorem [1]. Its ground state, however and at variance with the one-dimensional case, is ordered

for all spin values also in the antiferromagnetic case [2], and the model can hence be thought to have a phase transition at a critical temperature  $t_c(\pm 1, S) = 0 \forall S$ .

(ii) In the easy plane case, the Mermin-Wagner theorem still holds and no finite temperature transition towards a phase with a finite order parameter, may occur. However, a Berezinskii-Kosterlitz-Thouless (BKT) transition [3,4], related with the existence of vortex-like topological excitations, is known to characterize the class of the easy-plane models and may occur at a critical temperature  $t_{\text{BKT}}(\lambda, S) > 0$ .

The reference system for the easy-plane class is the *planar*, or *XY*, model, defined by Eq.(1) with  $\lambda = 0$ ,  $\mu = 1$ . Its BKT critical temperature has been seen to be finite for all spin values: above  $t_{\text{BKT}}$  the system is disordered, with exponentially decaying correlation functions. In the whole region  $0 < t < t_{\text{BKT}}$  the system is in a critical phase with vanishing magnetization: its correlation functions decay according to a power law, testifying to the existence of *quasi*-long-range order; at  $t = 0$  the magnetization gets a finite value and the system is ordered. The *XY* model may be thought to display two phase-transitions: a BKT one at a finite temperature, followed by one towards a fully ordered phase at  $t = 0$ .

(iii) In the easy-axis case, the Mermin-Wagner theorem does not hold, and the easy-axis models may undergo a transition of the Ising (I) type towards a phase with long-range order, at a critical temperature  $t_{\text{I}}(\mu, S) > 0$ .

The reference system for this class of models will be hereafter called the *Z* model, described by Eq.(1) with  $\mu = 0$ ,  $\lambda = 1$ ; such model has a transition temperature  $t_{\text{I}}(0, S) > 0$  for all spin values. Above  $t_{\text{I}}$  the system is in a paramagnetic phase, with exponentially decaying correlation functions; below  $t_{\text{I}}$  the system is ordered with a finite magnetization along the easy axis. The *Z* model with  $S = 1/2$  is the Ising model, representing an important source of information for the whole class of the easy-axis models, not only because of the existing exact results by Onsager [5], but also because of its fundamental role in the renormalization-group approach and in conformal field theory.

The information on the reference models, as well as the general considerations based on the symmetries of the Hamiltonian, are surely valuable, but not sufficient to fully appreciate the richness of features contained in Eq.(1), and to properly understand the thermodynamic and critical behaviour of the many existing real compounds whose magnetic behaviour is described by such Hamiltonian. To accomplish this goal one has to study how the specific values of  $\lambda$ ,  $\mu$ , and  $S$  may determine the behaviour of the system.

At a qualitative level, we know that quantum fluctuations, whose strength is measured by the quantum coupling  $1/S$ , introduce a disordering agent in the classical ( $S \rightarrow \infty$ ) picture: as a consequence, we expect the possible critical temperatures to decrease with decreasing  $S$ . The same effect is obtained by increasing  $|\lambda|$  (easy-plane case), or  $|\mu|$  (easy-axis case): this in fact means to weaken the anisotropic character of the system, thus allowing larger

spin fluctuations out of the easy plane or the easy axis, and inducing a lowering of the critical temperature. To this respect it is to be noticed that most real compounds have very weak anisotropies [6], i.e. values of  $\lambda$  or  $\mu$  very close to unity: this is the region where quantitative predictions are more difficult to obtain, as the model's character is not well defined and fluctuations are large.

Aim of this paper is to provide a quantitative description of the model (1) when  $S$  and  $\lambda$ , or  $\mu$ , are varied. We will mainly concentrate on the values of the critical temperatures, but also give expressions and results for other thermodynamic quantities. The method used is the pure-quantum self-consistent harmonic approximation (PQSCHA), extensively described in Ref. [7] and already applied to many magnetic systems (see for instance Refs. [8,9]). Its implementation is markedly different depending on the specific class of models considered, as explained in Section 2, and the easy-plane and easy-axis cases will be hence considered separately (in Section 3 and 4, respectively). In Section 5 we will comment on the resulting global picture and compare our results with all the available experimental and numerical simulation data. Conclusions about the critical behaviour of the models will be finally drawn in Section 6.

## 2 Method and spin-boson transformations

The PQSCHA is a semiclassical method based on the path-integral formulation of quantum statistical mechanics: the main peculiarity of the method is that of defining an analytical separation between classical and pure-quantum contributions to the thermodynamics of the system [10], thus allowing the possible exact treatment of the former, while requiring a self-consistent harmonic approximation of the latter. This means that the only approximated contribution is the non-linear pure-quantum one, which is in fact considered at the one-loop level. The value of such result is evident if one considers that most of the peculiar features of magnetic systems, including their critical behaviour, are determined by long-wavelength excitations, whose character is essentially classical; the possibility to fully take into account their non-linearity at the classical level, together with the fact that harmonic pure-quantum fluctuations are exactly considered, justifies the success of the PQSCHA in predicting most thermodynamic properties of magnetic systems in a large temperature range.

Without going into the details of the derivation of the PQSCHA, we report here the essential formulas, and discuss the scheme of implementation to magnetic systems, where differences between the sub-classes of models become essential.

Consider a quantum spin system on a lattice described by the Hamiltonian  $\hat{H}(\hat{\mathbf{S}})$  with  $\hat{\mathbf{S}} \equiv (\hat{\mathbf{S}}_1, \dots, \hat{\mathbf{S}}_N)$  and  $N$  number of lattice sites; if  $\hat{O}$  is the quantum operator relative to a physical observable of the system, the PQSCHA expression of its quantum statistical average has the clas-

sical-like form

$$\langle \hat{O} \rangle = \frac{1}{\mathcal{Z}_{\text{eff}}} \int d^N \mathbf{s} \mathcal{O}_{\text{eff}}(\mathbf{s}) e^{-\beta \mathcal{H}_{\text{eff}}(\mathbf{s})} \quad (2)$$

where  $\beta = t^{-1}$ ,  $\mathcal{Z}_{\text{eff}} = \int d^N \mathbf{s} e^{-\beta \mathcal{H}_{\text{eff}}}$ , and  $\mathbf{s} \equiv (\mathbf{s}_1, \dots, \mathbf{s}_N)$  with  $\mathbf{s}_i$  classical unit vectors. The effective Hamiltonian  $\mathcal{H}_{\text{eff}}(\mathbf{s}; t, S)$ , is a classical-like function, depending on the parameters of the original Hamiltonian, and determined by the PQSCHA renormalization procedure; a similar procedure, when applied to the quantum operator  $\hat{O}$ , leads to the function  $\mathcal{O}_{\text{eff}}(\mathbf{s}; t, S)$

The phase-space integral in Eq. (2) may be evaluated by any classical technique, such as the classical Monte Carlo (MC) simulation. Eq. (2), on the other hand, contains quantum renormalizations embodied in the temperature and spin dependence of  $\mathcal{H}_{\text{eff}}$  and  $\mathcal{O}_{\text{eff}}$ ; such dependence causes the effective classical model to change for each temperature point, so that *ad hoc* simulations must be performed, and only in very peculiar cases one can directly use existing MC data (see for instance the case of the isotropic model in Ref. [9]).

The PQSCHA naturally applies to bosonic systems, whose Hamiltonian is written in terms of conjugate operators  $\hat{q} \equiv (\hat{q}_1, \dots, \hat{q}_N)$ ,  $\hat{p} \equiv (\hat{p}_1, \dots, \hat{p}_N)$  such that  $[\hat{q}_m, \hat{p}_n] = i\delta_{mn}$ ; the method, however, does not require  $\hat{\mathcal{H}}(\hat{p}, \hat{q})$  to be standard, i.e. with separate quadratic kinetic  $\hat{p}$ -dependent and potential  $\hat{q}$ -dependent terms, and its application may be extended also to magnetic systems, according to the following scheme [10]: The spin Hamiltonian  $\hat{\mathcal{H}}(\mathbf{s})$  is mapped to  $\hat{\mathcal{H}}(\hat{p}, \hat{q})$  by a suitable spin-boson transformation; once the corresponding Weyl symbol  $\mathcal{H}(\underline{p}, \underline{q})$ , with  $\underline{p} \equiv (p_1, \dots, p_N)$  and  $\underline{q} \equiv (q_1, \dots, q_N)$  classical phase-space variables, has been determined [11], the PQSCHA renormalizations may be evaluated and  $\mathcal{H}_{\text{eff}}(\underline{p}, \underline{q})$  and  $\mathcal{O}_{\text{eff}}(\underline{p}, \underline{q})$  follow. Finally  $\mathcal{H}_{\text{eff}}(\mathbf{s})$  and  $\mathcal{O}_{\text{eff}}(\mathbf{s})$  are constructed by the inverse of the classical analogue of the spin-boson transformation used at the beginning.

In order to successfully carry out such renormalization scheme, the Weyl symbol of the bosonic Hamiltonian must be a well-behaved function in the whole phase space. Spin-boson transformations, on the other hand, can introduce singularities as a consequence of the topological impossibility of a global mapping of a spherical phase space into a flat one. The choice of the transformation must then be such that the singularities occur for configurations which are not thermodynamically relevant, and whose contribution may be hence approximated. Most of the methods for studying magnetic systems do in fact share this problem with the PQSCHA; what makes the difference is that by using the PQSCHA one separates the classical from the pure-quantum contribution to the thermal fluctuations, and the approximation only regards the latter, being the former exactly taken into account when the effective Hamiltonian is cast in the form of a classical spin Hamiltonian.

The spin-boson transformation which constitutes the first step of the magnetic PQSCHA is chosen according to

the symmetry properties of the original Hamiltonian and of its ground state.

In markedly easy-plane cases ( $|\lambda| \ll 1$ ) we use, for each spin operator, the Villain transformation (VT) [12]

$$\hat{S}^+ = e^{i\hat{q}} \sqrt{\tilde{S}^2 - \left(\hat{p} + \frac{1}{2}\right)^2}, \quad \hat{S}^- = (\hat{S}^+)^{\dagger}, \quad \hat{S}^z = \hat{p}; \quad (3)$$

this transformation keeps the  $O(2)$  symmetry in the easy plane, meanwhile allowing to deal with the square root in terms of a physically sound small- $\hat{p}$  approximation.

In the easy-axis case, it makes no sense to use Eqs.(3), as the expectation value of the  $z$ -component of each spin is now substantially different from zero. On the other hand, the Holstein-Primakoff transformation (HPT) [13]

$$\begin{aligned} \sqrt{2}\hat{S}^+ &= \sqrt{S + \tilde{S} - \hat{z}^2} (\hat{q} + i\hat{p}), \\ \hat{S}^- &= (\hat{S}^+)^{\dagger}, \quad \hat{S}^z = \tilde{S} - \hat{z}^2, \end{aligned} \quad (4)$$

and the Dyson-Maleev one (DMT) [14]

$$\begin{aligned} \sqrt{2}\hat{S}^+ &= \hat{q} + i\hat{p}, \quad \hat{S}^- = (\hat{q} - i\hat{p})(S + \tilde{S} - \hat{z}^2), \\ \hat{S}^z &= \tilde{S} - \hat{z}^2, \end{aligned} \quad (5)$$

with  $\hat{z}^2 \equiv (\hat{q}^2 + \hat{p}^2)/2$ , do both suggest the  $z$ -component to be the privileged one for alignment, thus fitting to the  $|\mu| < 1$  case.

The isotropic, or nearly isotropic, case is the most difficult to be treated, as no part of the spherical phase-space may be generically chosen to be described better than another; nevertheless, when the ground state is at least characterized by long-range order with an alignment axis, the HP and DM transformations are both seen to work well in the PQSCHA scheme. The reason is that the boson picture only serves to derive the pure-quantum renormalizations, while the symmetry is thereafter restored in  $\mathcal{H}_{\text{eff}}$  so that it is sufficient to assume a local alignment axis.

### 3 The easy-plane case

The Hamiltonian Eq. (1) in the easy-plane case takes the form

$$\hat{\mathcal{H}} = -J \sum_{\langle ij \rangle} \left[ \left( \hat{S}_i^x \hat{S}_j^x + \hat{S}_i^y \hat{S}_j^y \right) + \lambda \hat{S}_i^z \hat{S}_j^z \right] \quad (6)$$

with  $\lambda \in (-1, 1)$ . The antiferromagnetic sector is mapped in the  $\lambda \in (-1, 0]$  region of Eq. (6) by the canonical transformation  $(\hat{S}_i^x, \hat{S}_i^y, \hat{S}_i^z) \rightarrow \left( (-1)^i \hat{S}_i^x, (-1)^i \hat{S}_i^y, \hat{S}_i^z \right)$  where  $(-1)^i \equiv (-1)^{i_1+i_2}$ ; ferro- and antiferromagnets may be thus simultaneously studied.

The effective Hamiltonian relative to Eq. (6) is

$$\mathcal{H}_{\text{eff}} = -J \tilde{S}^2 j_{\text{eff}} \sum_{\langle ij \rangle} \left[ \left( s_i^x s_j^x + s_i^y s_j^y \right) + \lambda_{\text{eff}} s_i^z s_j^z \right] + \mathcal{G}, \quad (7)$$

where the renormalization parameters  $j_{\text{eff}}(t, \lambda, S)$ ,  $\lambda_{\text{eff}}(t, \lambda, S)$ , and  $\mathcal{G}(t, \lambda, S)$  have different expressions depending on the  $\lambda$ -region considered.

In the  $\lambda \ll 1$  case, the VT Eqs. (3) may be safely used, and give [15]

$$j_{\text{eff}}^{\text{V}} = \left(1 - \frac{1}{2}D_{\perp}\right)^2 e^{-\mathcal{D}_{\parallel}/2}, \quad (8)$$

$$\lambda_{\text{eff}}^{\text{V}} = \lambda \left(1 - \frac{1}{2}D_{\perp}\right)^{-1} e^{\mathcal{D}_{\parallel}/2}, \quad (9)$$

$$\mathcal{G}^{\text{V}} = J\tilde{S}^2 N \left[ t\Gamma - \frac{t}{2} \ln \left(1 - \frac{1}{2}D_{\perp}\right) - \Theta^{\text{V}} \right], \quad (10)$$

where the renormalization coefficients  $D_{\perp}$  and  $\mathcal{D}_{\parallel}$  represent the effects of in-plane and out-of-plane pure-quantum fluctuations, respectively, and have the form

$$D_{\perp} = \frac{1}{2\tilde{S}N} \sum_{\mathbf{k}} \frac{b_{\mathbf{k}}}{a_{\mathbf{k}}} \mathcal{L}_{\mathbf{k}}, \quad (11)$$

$$\mathcal{D}_{\parallel} = \frac{1}{2\tilde{S}N} \sum_{\mathbf{k}} (1 - \gamma_{\mathbf{k}}) \frac{a_{\mathbf{k}}}{b_{\mathbf{k}}} \mathcal{L}_{\mathbf{k}}, \quad (12)$$

with

$$a_{\mathbf{k}}^2 = 4e^{-\mathcal{D}_{\parallel}/2} (1 - \lambda_{\text{eff}} \gamma_{\mathbf{k}}), \quad (13)$$

$$b_{\mathbf{k}}^2 = 4 \left(1 - \frac{1}{2}D_{\perp}\right)^2 e^{-\mathcal{D}_{\parallel}/2} (1 - \gamma_{\mathbf{k}}), \quad (14)$$

$\mathcal{L}_{\mathbf{k}} = (\coth f_{\mathbf{k}} - 1/f_{\mathbf{k}})$ ,  $\Gamma = N^{-1} \sum_{\mathbf{k}} \ln(\sinh f_{\mathbf{k}}/f_{\mathbf{k}})$ ,  $f_{\mathbf{k}} = a_{\mathbf{k}} b_{\mathbf{k}} / (2\tilde{S}t)$ ,  $\gamma_{\mathbf{k}} = \sum_{\mathbf{d}} \cos(\mathbf{k} \cdot \mathbf{d}) / 4$ ,  $\mathbf{d} = (\pm 1, \pm 1)$ , and  $\mathbf{k}$  is a wave vector in the first Brillouin zone. The uniform coefficient  $\Theta^{\text{V}}$  is

$$\Theta^{\text{V}} = e^{-\mathcal{D}_{\parallel}/2} (2D_{\perp} + (1 - D_{\perp})\mathcal{D}_{\parallel}).$$

Close to the isotropic limit,  $\lambda \lesssim 1$ , the HPT must be used: because of the residual easy-plane character of the model, the privileged axis, i.e. the quantization one, must be chosen in the easy plane; in particular, we choose the  $y$  direction as the local alignment one. A quite complicated PQSCHA implementation finally leads to the following expressions [16]:

$$j_{\text{eff}}^{\text{HP}} = \theta^4, \quad (15)$$

$$\lambda_{\text{eff}}^{\text{HP}} = \lambda + \frac{d}{\theta^2} (1 - \lambda) + \frac{D^{pp}}{\theta^2} (1 - \lambda)^2, \quad (16)$$

$$\mathcal{G}^{\text{HP}} = J\tilde{S}^2 N \left[ t\Gamma + \frac{\theta^2}{N\tilde{S}} \sum_{\mathbf{k}} a_{\mathbf{k}} b_{\mathbf{k}} \mathcal{L}_{\mathbf{k}} - \Theta^{\text{HP}} \right], \quad (17)$$

where the temperature and spin dependent renormalization coefficients are defined as follows:

$$\theta^2 = 1 - \frac{1}{2}\mathcal{D} + \frac{1}{2}d, \quad d = \frac{1}{2}(D^{qq} - \lambda_{\text{eff}} D^{pp}), \quad (18)$$

$$\mathcal{D} = \frac{1}{N\tilde{S}} \sum_{\mathbf{k}} (1 - \gamma_{\mathbf{k}}) \frac{a_{\mathbf{k}}}{b_{\mathbf{k}}} \mathcal{L}_{\mathbf{k}}, \quad (19)$$

and

$$D^{pp} = \frac{1}{2\tilde{S}N} \sum_{\mathbf{k}} \frac{a_{\mathbf{k}}}{b_{\mathbf{k}}} \gamma_{\mathbf{k}} \mathcal{L}_{\mathbf{k}}, \quad D^{qq} = \frac{1}{2\tilde{S}N} \sum_{\mathbf{k}} \frac{b_{\mathbf{k}}}{a_{\mathbf{k}}} \gamma_{\mathbf{k}} \mathcal{L}_{\mathbf{k}},$$

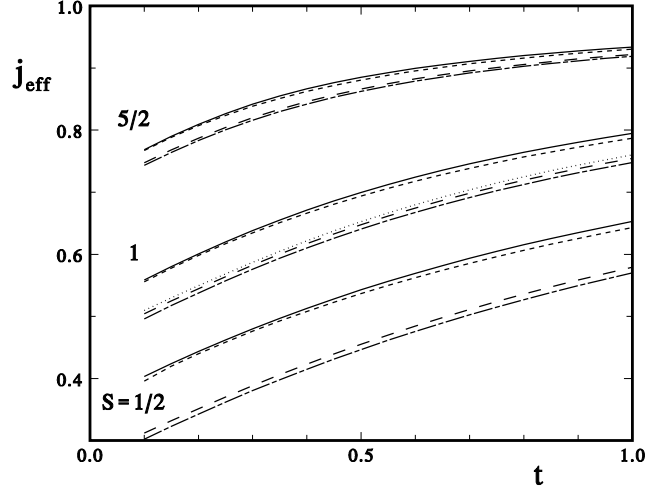


**Fig. 1.** Renormalization parameter  $j_{\text{eff}}$  vs  $t$  for the easy-plane model with  $\lambda = 0$  (full curve), 0.5 (dashed), 0.7 (long-dashed), 0.9 (dash-dotted), and  $S = 1/2, 1, 5/2$ . The dotted line is  $j_{\text{eff}}$  for  $S = 1, \lambda = 0.5$ , as obtained by the HPT.

with dimensionless frequencies

$$a_{\mathbf{k}}^2 = 4\theta^2 (1 - \lambda_{\text{eff}} \gamma_{\mathbf{k}}), \quad (20)$$

$$b_{\mathbf{k}}^2 = 4\theta^2 (1 - \gamma_{\mathbf{k}}). \quad (21)$$

The uniform coefficient  $\Theta^{\text{HP}}$  is

$$\Theta^{\text{HP}} = D^{qq} (1 - 3D^q - D^p) + \lambda D^{pp} (3 - 3D^p - D^q) + 2(D^{qq})^2 + 2(D^{pp})^2 - (D^q + D^p)^2 + 2(D^q + D^p),$$

with

$$D^p = \frac{1}{2\tilde{S}N} \sum_{\mathbf{k}} \frac{a_{\mathbf{k}}}{b_{\mathbf{k}}} \mathcal{L}_{\mathbf{k}}, \quad D^q = \frac{1}{2\tilde{S}N} \sum_{\mathbf{k}} \frac{b_{\mathbf{k}}}{a_{\mathbf{k}}} \mathcal{L}_{\mathbf{k}}.$$

The renormalization of the exchange energy by the factor  $j_{\text{eff}} < 1$ , and the weakening of the easy-plane anisotropy ( $|\lambda| \leq |\lambda_{\text{eff}}|$ ), are seen to be, both for strong and weak anisotropy, the result of the cooperative effect of in-plane and out-of plane pure-quantum fluctuations. It is worthwhile noticing that, in the isotropic limit  $|\lambda| = 1$ , the effective Hamiltonian (7), determined by the HPT, coincides with the one found directly for the isotropic model by the DMT.

In Fig. 1 we show the renormalization parameters  $j_{\text{eff}}$  vs.  $t$ , for different values of  $S$  and  $\lambda$ ; the two most (least) anisotropic cases are treated by the VT (HPT). For  $S = 1$  and  $\lambda = 0.5$ ,  $j_{\text{eff}}$  as obtained by the HPT is also shown (dotted line): the difference with the VT result (dashed line) is remarkable, testifying that both transformations cannot give very accurate results in such intermediate region. However, as we will see in Section 5, this does not dramatically affect the critical temperature estimation.

The difference  $(\lambda_{\text{eff}} - \lambda)$  is shown in Fig. 2 as a function of  $\lambda$ , for different values of  $S$  and  $t$ . For each couple  $(t, S)$

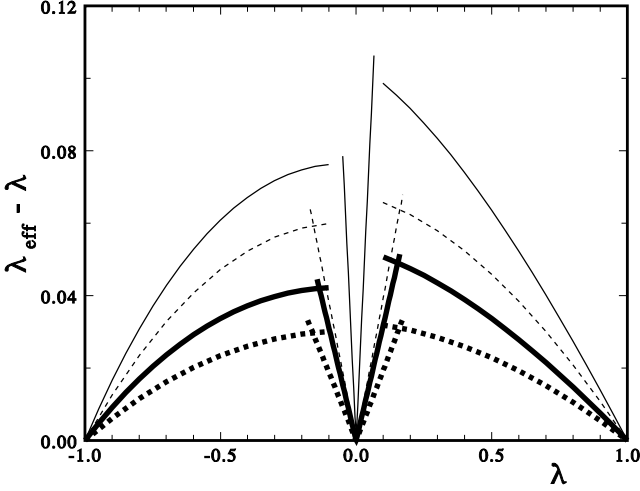


**Fig. 2.** Difference  $(\lambda_{\text{eff}} - \lambda)$  vs  $\lambda$  for the easy-plane model with  $S = 1/2$  (thin) and 1 (thick), at  $t = 0.5$  (full) and 1 (dashed). For each  $t$  and  $S$ , both the HP (curves passing through  $(\pm 1, 0)$ ) and the V (curves passing through the origin) results are shown.

the curves passing through the origin are obtained by the VT, while those passing through the point  $(-1, 0)$  or  $(1, 0)$  are obtained by the HPT in the antiferro- or ferromagnetic case, respectively; the two types of results do not smoothly connect to each other, but nevertheless cover the whole  $[-1, 1]$  interval and show a behaviour of the same type of that found in the easy-axis case (see Fig.5), where the problem of using two different spin boson transformations is not present. As expected, the HP curves display the correct  $|\lambda| \rightarrow 1$  behaviour (i.e.  $|\lambda_{\text{eff}}|^{\text{HP}} \rightarrow 1$ ), while  $\lambda_{\text{eff}}^{\text{V}}$  is seen to be proportional to  $\lambda$ , when  $\lambda \rightarrow 0$ .

As mentioned in the Introduction, the easy-plane models are characterized by a critical phase, with vanishing magnetization and diverging correlation length, extending in the temperature region  $0 < t < t_{\text{BKT}}$ ; thermodynamic quantities that may be significantly studied in such phase are, for instance, the free energy and the specific heat. To this respect, notice that the uniform term  $\mathcal{G}$ , Eqs. (10) and (17), not entering the statistical averages' calculation, is essential in the evaluation of the partition function  $\mathcal{Z}$ .

In the paramagnetic phase  $t > t_{\text{BKT}}$ , one of the fundamental thermodynamic quantities to be investigated, is the in-plane correlation length defined by the asymptotic behaviour of the correlation functions

$$G(r) \equiv \frac{\eta_{\mathbf{r}}}{S^2} \langle \hat{S}_{\mathbf{i}}^x \hat{S}_{\mathbf{i}+\mathbf{r}}^x + \hat{S}_{\mathbf{i}}^y \hat{S}_{\mathbf{i}+\mathbf{r}}^y \rangle_{r \rightarrow \infty} \sim e^{-\frac{r}{\xi}} \quad (22)$$

with  $\mathbf{r} = (r_1, r_2)$  any vector on the square lattice,  $r \equiv |\mathbf{r}|$  and  $\eta_{\mathbf{r}} = 1$  or  $(-1)^{r_1+r_2}$  in the ferro- or antiferromagnetic case.

By using Eq. (2) the following PQSCHA expression is found

$$G(r) = \Delta_{\mathbf{r}} \langle s_{\mathbf{i}}^x s_{\mathbf{i}+\mathbf{r}}^x + s_{\mathbf{i}}^y s_{\mathbf{i}+\mathbf{r}}^y \rangle_{\text{eff}} , \quad (23)$$

where  $\langle \cdot \rangle_{\text{eff}} \equiv \mathcal{Z}^{-1} \int d^N \mathbf{s}(\cdot) e^{-\beta \mathcal{H}_{\text{eff}}}$  is the classical-like statistical average defined by the effective Hamiltonian.

When the VT is used, i.e. in the strongly easy-plane case, Eq. (23) holds for all values of  $r$ , with

$$\Delta_{\mathbf{r}}^{\text{VT}} = \left(1 - \frac{1}{2} \mathcal{D}_{\perp}\right)^2 e^{-\mathcal{D}_{\parallel}/2} e^{-D_{\mathbf{r}}} , \quad (24)$$

and

$$D_{\mathbf{r}} = \frac{1}{\tilde{S}N} \sum_{\mathbf{k}} \frac{a_{\mathbf{k}}}{b_{\mathbf{k}}} \cos(\mathbf{k} \cdot \mathbf{r}) \mathcal{L}_{\mathbf{k}} .$$

In the nearly isotropic region, the use of the HPT leads to a much more complicated general expression for  $G(r)$ , that nonetheless goes to expression (23) with coefficient

$$\Delta_{\mathbf{r}}^{\text{HP}} \rightarrow \left(1 - \frac{1}{2}(D^q + D^p)\right) \left(1 - \frac{1}{8}(5D^q + 3D^p)\right) , \quad (25)$$

for large  $r$ . From Eqs. (24) and (25), the renormalization coefficient  $\Delta_{\mathbf{r}}$  is seen to converge to a finite value when  $r \rightarrow \infty$ ; this property, as we will see in Section 5, is of fundamental importance when the critical behaviour of the model is under investigation. In particular it means that the correlation length of the quantum model is related with that of its classical counterpart by the relation

$$\xi(t, \lambda, S) = \xi^{\text{cl}}(t_{\text{eff}}, \lambda_{\text{eff}}) \quad (26)$$

with  $t_{\text{eff}} \equiv t/j_{\text{eff}}$ . This relation allows us to evaluate the correlation length of a quantum model with spin  $S$ , at a given temperature  $t$ , by performing a classical MC simulation on a model with anisotropy  $\lambda_{\text{eff}}$ , at the effective temperature  $t_{\text{eff}}$ ; a particularly simple case is that of the XY model  $\lambda = \lambda_{\text{eff}} = 0$ , whose correlation length may be directly determined in terms of the classical one, by a simple temperature scaling. Fig. 3 shows the correlation length versus  $t$ , for  $S = 1$  and  $\lambda = 0, -0.5, -0.999$ , and  $-1$ . The classical MC data for  $\lambda = 0$  and  $\lambda = 0.999$ , Refs. [17] and [16] respectively, are also shown.

## 4 The easy-axis case

The Hamiltonian Eq. (1) in the easy-axis case takes the form

$$\hat{\mathcal{H}} = -J \sum_{\langle \mathbf{i}, \mathbf{j} \rangle} \left[ \mu \left( \lambda \hat{S}_{\mathbf{i}}^x \hat{S}_{\mathbf{j}}^x + \hat{S}_{\mathbf{i}}^y \hat{S}_{\mathbf{j}}^y \right) + \hat{S}_{\mathbf{i}}^z \hat{S}_{\mathbf{j}}^z \right] \quad (27)$$

with  $\mu \in (-1, 1)$  and  $\lambda = \text{sign}(\mu)$ . The antiferromagnetic sector is mapped in the  $\mu \in (-1, 0]$  region of Eq. (27) by the canonical transformation  $(\hat{S}_{\mathbf{i}}^x, \hat{S}_{\mathbf{i}}^y, \hat{S}_{\mathbf{i}}^z) \rightarrow ((-1)^{\mathbf{i}} \hat{S}_{\mathbf{i}}^x, \hat{S}_{\mathbf{i}}^y, (-1)^{\mathbf{i}} \hat{S}_{\mathbf{i}}^z)$ . Because of the easy-axis character of the model, the HP and DM transformations may be safely used, and actually give the same results; the latter, however, may be preferred because of its simpler structure.

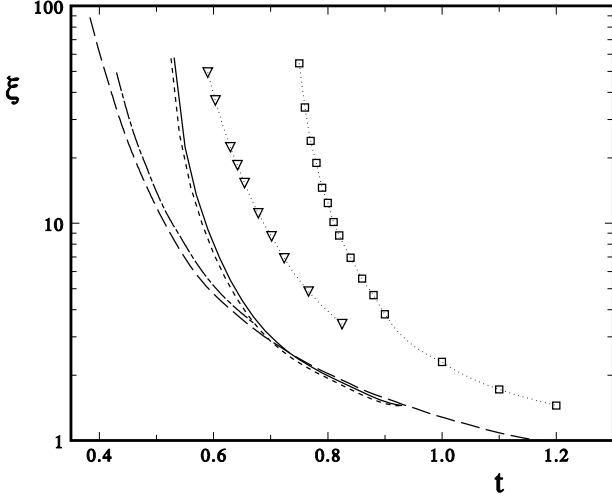


**Fig. 3.** Correlation length  $\xi$  vs  $t$  for the easy-plane model with  $S = 1$  and  $\lambda = 0$  (full),  $-0.5$  (dashed),  $-0.999$  (dash-dotted), and  $-1$  (long-dashed). Symbols are classical MC data for  $\lambda = 0$  (squares [17]) and  $\lambda = 0.999$  (triangles [16]).

The PQSCHA effective Hamiltonian relative to Eq.(27) is found to be [18]

$$\mathcal{H}_{\text{eff}} = -J\tilde{S}^2 j_{\text{eff}} \sum_{\langle ij \rangle} \left[ \mu_{\text{eff}} \left( \lambda s_i^x s_j^x + s_i^y s_j^y \right) + s_i^z s_j^z \right] + \mathcal{G}, \quad (28)$$

where  $j_{\text{eff}}(t, \mu, S)$ ,  $\mu_{\text{eff}}(t, \mu, S)$ , and  $\mathcal{G}(t, \mu, S)$  are

$$j_{\text{eff}} = \theta_{\parallel}^4, \quad \mu_{\text{eff}} = \mu \frac{\theta_{\perp}^2}{\theta_{\parallel}^2}, \quad (29)$$

$$\mathcal{G} = 2J\tilde{S}^2(1 - \theta_{\parallel}^4) + J\tilde{S}^2\Gamma, \quad (30)$$

with

$$\theta_{\parallel}^2 = 1 - \frac{\mathcal{D}_{\parallel}}{2}, \quad \theta_{\perp}^2 = 1 - \frac{\mathcal{D}_{\perp}}{2}, \quad (31)$$

$$\Gamma = t \sum_{\mathbf{k}} \ln \left( \frac{\sinh f_{\mathbf{k}}}{\theta_{\perp}^2 f_{\mathbf{k}}} \right), \quad (32)$$

and the coefficients

$$\begin{aligned} \mathcal{D}_{\parallel} &= \frac{1}{N\tilde{S}} \sum_{\mathbf{k}} \frac{a_{\mathbf{k}}}{b_{\mathbf{k}}} (1 - \mu\lambda\gamma_{\mathbf{k}}) \mathcal{L}_{\mathbf{k}}, \\ \mathcal{D}_{\perp} &= \frac{1}{N\tilde{S}} \sum_{\mathbf{k}} \frac{a_{\mathbf{k}}}{b_{\mathbf{k}}} \left( 1 - \frac{\gamma_{\mathbf{k}}}{\mu\lambda} \right) \mathcal{L}_{\mathbf{k}} \end{aligned} \quad (33)$$

are self-consistently determined by solving Eqs. (31) and (33), with dimensionless frequencies

$$a_{\mathbf{k}}^2 = 4 \left( \theta_{\parallel}^2 - \mu\theta_{\perp}^2\gamma_{\mathbf{k}} \right), \quad (34)$$

$$b_{\mathbf{k}}^2 = 4 \left( \theta_{\parallel}^2 - \mu\lambda\theta_{\perp}^2\gamma_{\mathbf{k}} \right). \quad (35)$$

As in the easy-plane case, quantum renormalizations weaken both the energy scale ( $j_{\text{eff}} < 1$ ) and the anisotropy

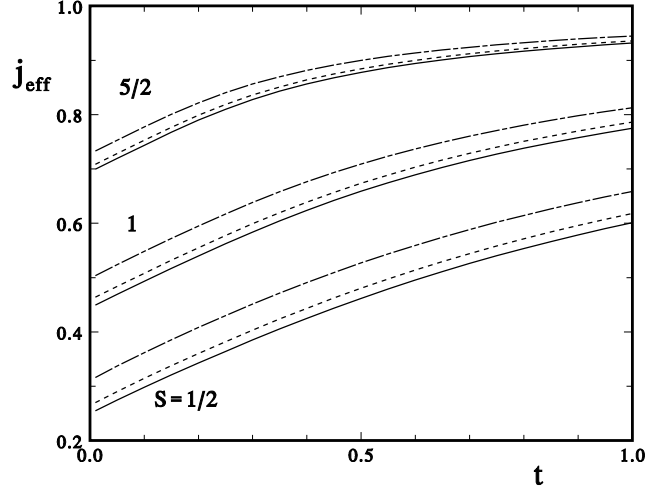


**Fig. 4.** Renormalization parameter  $j_{\text{eff}}$  vs  $t$  for the easy-axis model with  $\mu = 0$  (full),  $0.5$  (dashed),  $0.9$  (dash-dotted), and  $S = 1/2, 1, 5/2$ .

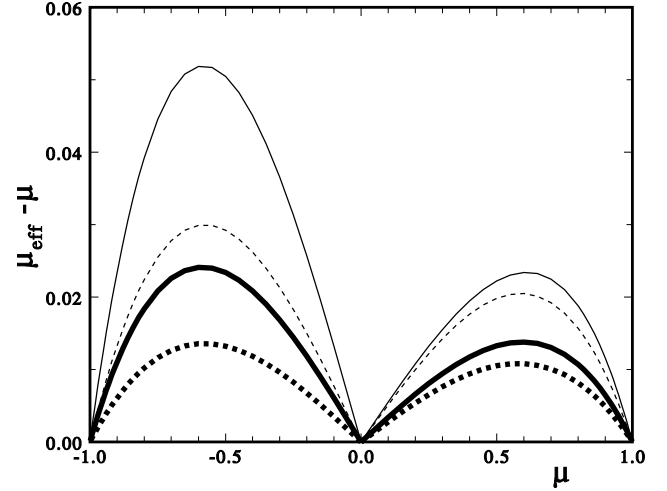


**Fig. 5.** Difference  $(\mu_{\text{eff}} - \mu)$  vs  $\mu$  for the easy-axis model with  $S = 1/2$  (thin) and  $1$  (thick), at  $t = 0.5$  (full) and  $1$  (dashed).

( $|\mu_{\text{eff}}| > \mu$ ). In Fig. 4 we show the renormalization parameter  $j_{\text{eff}}$  vs.  $t$  for different values of  $S$  and  $\mu$ . In Fig. 5, where the difference  $\mu_{\text{eff}} - \mu$  is shown as a function of  $\mu$ , we see that, at variance with the easy-plane case (see Fig. 2), the almost isotropic regime is smoothly connected with the strongly axial one, testifying to the suitability of the DMT in treating the whole easy-axis subclass of models.

When  $\mu$  vanishes the renormalization coefficient  $\mathcal{D}_{\perp}$  may be shown to keep finite, so that  $\mu_{\text{eff}} \rightarrow 0$ , and the  $Z$  model, with a single optical mode  $a_{\mathbf{k}}^2 = b_{\mathbf{k}}^2 = 4\theta_{\parallel}^2$ ,  $\forall \mathbf{k}$ , is recovered; for  $S = 1/2$  such model coincides with the Ising one.

The easy-axis case is characterized by a finite temperature phase-transition towards a fully ordered phase;

many thermodynamic properties may be hence studied both above and below the critical temperature  $t_I$ , and, in particular, the PQSCHA expression for the magnetization along the easy axis  $m \equiv \sum_i \eta_i \langle \hat{S}_i^z \rangle / N \tilde{S}$  is

$$m = \theta_{\parallel}^2 \langle s_{\mathbf{i}}^z \rangle_{\text{eff}} . \quad (36)$$

The most significant quantity in the paramagnetic phase  $t > t_I$  is the correlation length, here defined by the asymptotic behaviour of the isotropic correlation functions

$$G(r) \equiv \frac{\eta_{\mathbf{r}}}{\tilde{S}^2} \langle \hat{\mathbf{S}}_{\mathbf{i}} \cdot \hat{\mathbf{S}}_{\mathbf{i}+\mathbf{r}} \rangle \underset{r \rightarrow \infty}{\sim} e^{-\frac{r}{\xi}} ; \quad (37)$$

the PQSCHA expression for  $G(r)$  is

$$G(r) = \theta_{\mathbf{r}}^4 \langle \mathbf{s}_{\mathbf{i}} \cdot \mathbf{s}_{\mathbf{i}+\mathbf{r}} \rangle_{\text{eff}} , \quad (38)$$

where  $\theta_{\mathbf{r}}^2 = 1 - \mathcal{D}_{\mathbf{r}}/2$  and

$$\mathcal{D}_{\mathbf{r}} = \frac{1}{N \tilde{S}} \sum_{\mathbf{k}} \frac{a_{\mathbf{k}}}{b_{\mathbf{k}}} (1 - \cos(\mathbf{k} \cdot \mathbf{r})) \mathcal{L}_{\mathbf{k}}$$

is a further site-dependent renormalization coefficient. For increasing  $r$ , as in the easy-plane case, the coefficient  $\theta_{\mathbf{r}}^4$  keeps finite and rapidly converges to a uniform term: the asymptotic behaviour of  $G(r)$  is hence determined by that of the classical-like correlation functions  $\langle \mathbf{s}_{\mathbf{i}} \cdot \mathbf{s}_{\mathbf{i}+\mathbf{r}} \rangle_{\text{eff}}$ , and the relation

$$\xi(t, \mu, S) = \xi^{\text{cl}}(t_{\text{eff}}, \mu_{\text{eff}}) \quad (39)$$

may be used. As in the easy-plane case, results for the quantum reference ( $Z$ ) model are obtained by a simple temperature scaling of the classical data; we have hence performed MC simulations on the classical  $Z$  model, and produced results for the quantum model with  $S = 1/2, 1$  and  $5/2$ . The corresponding magnetization and correlation-length curves are shown in Figs.6 and 7, respectively. As for the latter, notice the much sharper divergence with respect to the  $XY$  model (compare the dashed curve in Fig.7 with the full curve of Fig.3).

## 5 Transition temperatures

The PQSCHA expressions for the effective Hamiltonian and the correlation functions contain two essential pieces of information: (a) the effective Hamiltonian keeps the symmetry properties of the original quantum model; (b) the quantum correlation functions share the asymptotic behaviour with their classical counterpart. These two statements not only lead us to the relations (26) and (39), but also allow us to assert that the critical behaviour of the quantum model is that of its effective classical counterpart, and that, for the critical temperature, the relation

$$t_c(\nu, S) = j_{\text{eff}}(t_c, \nu, S) t_c^{\text{cl}}(\nu_{\text{eff}}(t_c, \nu, S)) \quad (40)$$

holds.

Due to the temperature dependence of  $j_{\text{eff}}$  and  $\nu_{\text{eff}}$ , Eq. (40) is quite involute; it may be nonetheless numerically solved if an analytical expression for  $t_c^{\text{cl}}(\nu)$  is available. Such expression does not actually exist, neither in

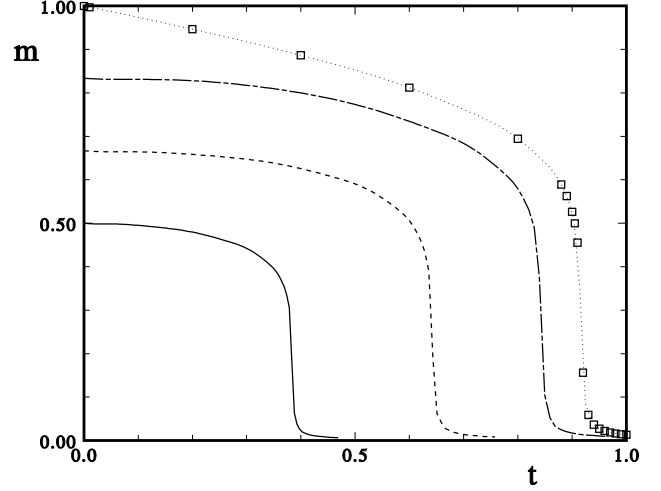


**Fig. 6.** Magnetization curves for the  $Z$  model with  $S = 1/2$  (full), 1 (dashed),  $5/2$  (dash-dotted), and  $\infty$  (dotted); symbols are our classical MC data.

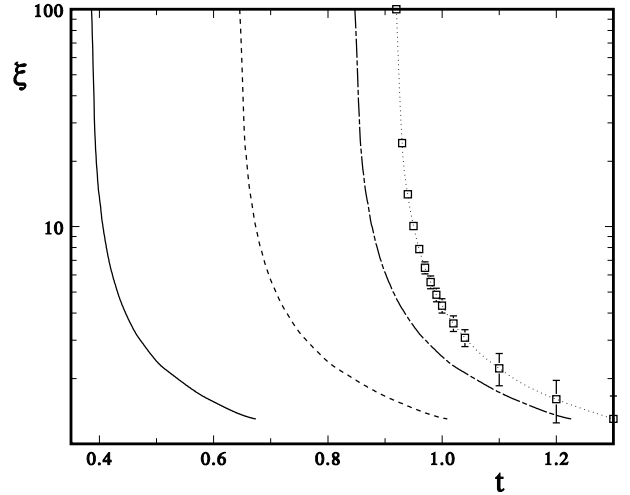


**Fig. 7.** Correlation length for the  $Z$  model with  $S = 1/2, 1, 5/2$ , and  $\infty$  (curves and symbols as in previous figure).

the easy-plane nor in the easy-axis case; we have hence collected a set of classical MC data properly distributed in the  $[0, 1)$  interval, in order to determine a precise interpolating function  $\tau_c^{\text{cl}}(\nu)$ .

In the easy-plane case, classical MC data have been taken from Ref. [17] and interpolated by the function

$$\tau_{\text{BKT}}^{\text{cl}}(\lambda) = a (1 + b\lambda^2 + c\lambda^4 - d \ln(1 - \lambda^2))^{-1} , \quad (41)$$

$$a = 0.695 , \quad b = -0.012 , \quad c = 0.032 , \quad d = 0.0648 ,$$

where the  $\lambda \rightarrow -\lambda$  invariance has been imposed.

In the easy-axis case, sources of the classical MC data have been Refs. [19] and [20], as well as our new data  $t_I^{\text{cl}}(0.5) = 0.88 \pm 0.01$  and  $t_I^{\text{cl}}(0.8) = 0.81 \pm 0.01$ ; the re-

sulting interpolating function is

$$\tau_I^{\text{cl}}(\mu) = a(1 + b\mu^2 + c\mu^4 - d\ln(1 - \mu^2))^{-1}, \quad (42)$$

$$a = 0.917, \quad b = 0.068, \quad c = 0.097, \quad d = 0.0636,$$

where, again, the constraint  $t_I^{\text{cl}}(\mu) = t_I^{\text{cl}}(-\mu)$  has been imposed.

Equations (41) and (42) should only be considered as reasonable interpolating functions of the available data; in particular, they do not reproduce the correct asymptotic behaviour in the  $\nu \rightarrow 1$  isotropic limit. Such asymptotic behaviours, on the other hand, are not accessible by numerical techniques and are actually determined by Renormalization-Group approaches. However, all of the numerical and experimental data are in the  $\nu$ -region where  $t_c(\nu)$  is sensibly different from zero, as seen in Figs. 8 and 9, i.e. where the above mentioned asymptotic behaviours have not set in yet.

Once  $t_c^{\text{cl}}(\nu) \simeq \tau_c^{\text{cl}}(\nu)$  has been determined, Eq. (40) may be numerically solved thus giving the value of the quantum critical temperature, for any value of  $\nu$  and  $S$ , in a few seconds on a standard PC.

In Fig. 8 we show the resulting curves for  $S = 1/2$ , 1, 5/2, and  $\infty$  in the easy-plane case: for each spin, the whole  $(-1, 1)$  interval is covered by two different types of curves, corresponding to the use of  $j_{\text{eff}}^{\text{V},\lambda_{\text{eff}}^{\text{V}}}$  and  $j_{\text{eff}}^{\text{HP},\lambda_{\text{eff}}^{\text{HP}}}$  in the strongly easy-plane and nearly isotropic regions, respectively. The available quantum MC data [21,22] are also shown, and agree very well with our results, despite being in the region where, because of the strong quantum fluctuations, the use of the PQSCHA becomes more delicate; unfortunately no experimental data exist, to our knowledge, for  $t_{\text{BKT}}$ .

In Fig. 9 the transition temperature  $t_I(\mu, S)$  is shown for  $S = 1/2$ , 1, 5/2, and  $\infty$ ; in this case, there exist several experimental data, for the real compounds  $\text{K}_2\text{NiF}_4$  ( $\mu = -0.996$ ,  $S = 1$ ,  $t_I^{\text{exp}} = 0.416$ ) [23,24],  $\text{Rb}_2\text{NiF}_4$  ( $\mu = -0.982$ ,  $S = 1$ ,  $t_I^{\text{exp}} = 0.477$ ) [25],  $\text{K}_2\text{MnF}_4$  ( $\mu = -0.995$ ,  $S = 5/2$ ,  $t_I^{\text{exp}} = 0.553$ ) [23,26],  $\text{Rb}_2\text{MnCl}_4$  ( $\mu = -0.997$ ,  $S = 5/2$ ,  $t_I^{\text{exp}} = 0.558$ ) [27], and  $\text{Rb}_2\text{MnF}_4$  ( $\mu = -0.994$ ,  $S = 5/2$ ,  $t_I^{\text{exp}} = 0.575$ ) [23,28], whose agreement with our results is very good, despite being in the most difficult region to be studied, i.e. in the nearly isotropic one.

The  $S = 1/2$  easy-axis antiferromagnetic case deserves a few more comments, as a quite well distributed scan of the  $\mu \in [-1, 0)$  region may be performed by putting together the exact result for the Ising model [5],  $t_I(0, 1/2) = 0.567$ , the quantum MC data by Ding [29],  $t_I(0.5, 1/2) = 0.5$ ,  $t_I(0.99, 1/2) = 0.298$ , and the experimental data for the real compound  $\text{YBa}_2\text{Cu}_3\text{O}_{6.1}$  ( $\mu \simeq 0.992$ ,  $S = 1/2$ ,  $t_I^{\text{exp}} = 0.310$ ) [30]. As for the PQSCHA, we know that its results are quantitatively reliable if quantum renormalizations are not too strong: a reasonable criterion to check whether such condition is fulfilled or not is to require  $j_{\text{eff}} \gtrsim 0.5$ , meaning a quantum renormalizations of the energy scale of about 50%. Such criterion, as seen in Fig. 4, is not satisfied for  $S = 1/2$  and  $t \leq 0.5$ : our  $t_I(\mu, 1/2)$  curve does in fact underestimate the most anisotropic numerical and experimental data, despite displaying the correct qualitative behaviour. A significant improvement may be

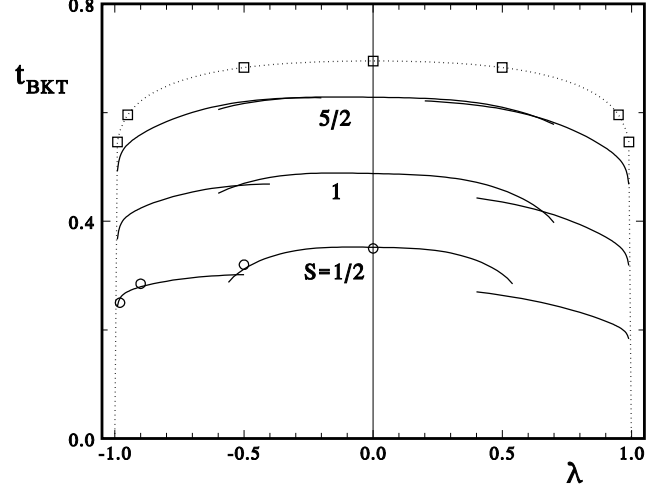


**Fig. 8.** BKT critical temperature *vs*  $\lambda$  for the easy-plane model with  $S = 1/2, 1, 5/2$ . Symbols are the quantum MC data for  $S = 1/2$  (circles [21,22]), and the classical MC data (squares [17]) used to construct  $\tau_{\text{BKT}}^{\text{cl}}(\lambda)$ , shown as dotted line.

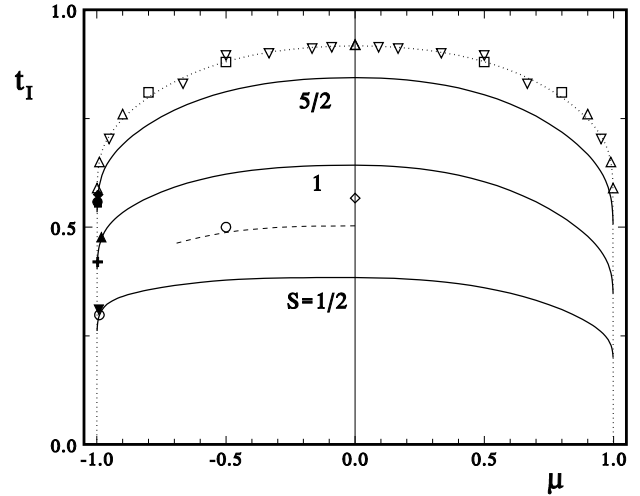


**Fig. 9.** Ising critical temperature *vs*  $\mu$  for the easy-axis model with  $S = 1/2, 1, 5/2$ . Symbols are quantum MC data [29] for  $S = 1/2$  (open circles), experimental data (filled symbols) for several real compounds (see Fig.10 for details), and the classical MC data (upwards triangles [20], downwards triangles [19], circles from our new simulations) used to construct  $\tau_I^{\text{cl}}(\mu)$ , shown as dotted line; the open diamond is the exact result for the Ising model; see text for the dashed line.

obtained by using the PQSCHA with the modified Low Coupling Approximation, as defined in Ref. [9], whose results are shown by the dashed line. This modified version of the method has the disadvantage, however, of not being capable to cover the whole  $(-1, 1)$   $\mu$ -interval, because of the loss of solution of its self-consistent equations when

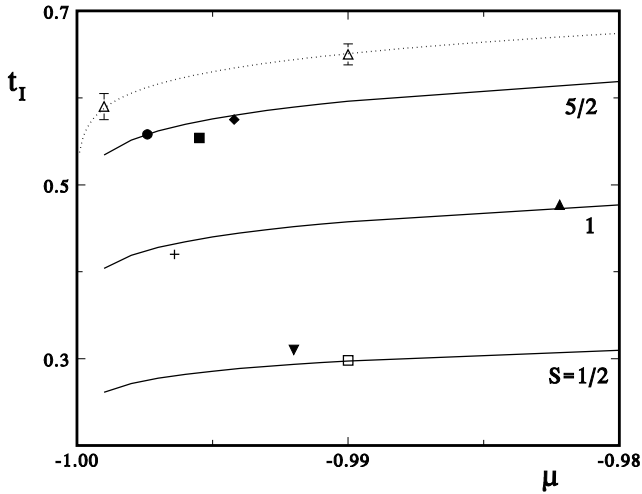


**Fig. 10.** Ising critical temperature for the antiferromagnetic easy-axis model, near the isotropic limit. Curves and open symbols are as in Fig.9; Filled symbols are experimental data for the compounds  $\text{YBa}_2\text{Cu}_3\text{O}_{6.1}$  (downwards triangle),  $\text{K}_2\text{NiF}_4$  (cross),  $\text{Rb}_2\text{NiF}_4$  (upwards triangle),  $\text{Rb}_2\text{MnCl}_4$  (circle),  $\text{Rb}_2\text{MnF}_4$  (diamond); see text for references.

moving towards the isotropic limit (reason for the dashed curve in Fig. 9 to be interrupted).

On the other hand, the almost isotropic region, which is the most interesting from the experimental point of view, is well described by our results, even for  $S = 1/2$ , as seen in Fig. 10.

## 6 Conclusions

The results found by the PQSCHA for the 2d Heisenberg antiferromagnets with easy-plane or easy-axis anisotropy, show that quantum fluctuations introduce temperature, anisotropy, and spin dependent renormalizations of both the energy scale and the anisotropy of the model, consequently reducing the temperature at which a phase transition, of the BKT or Ising type, is expected. Such reduction, however, is never seen to push the critical temperature down to zero, so that the whole class of quantum models described by Eq. (1) with  $|\mu| \neq |\lambda|$  turns out to be characterized by a finite temperature transition.

In Fig.11 a global picture of the situation is visualized by the  $t_c$  curves for different spin values, versus the ratio  $\lambda/\mu$ : the central region corresponds to the easy-plane case, while the two external branches represents the easy-axis ferro- and antiferromagnetic cases. The  $t_c$  reduction is seen to be more marked for small spin and in the ferromagnetic case, thus leading to the conclusion that, should  $t_c$  vanish for some critical  $\nu_c(S)$ , we expect  $|\nu_c(S)|$  to be an increasing function of  $S$  which is larger in the antiferromagnetic case, and such that its difference from unity is less than  $10^{-2}$ . In the  $S = 1/2$  case, despite being the one for which the PQSCHA is less precise, our picture com-

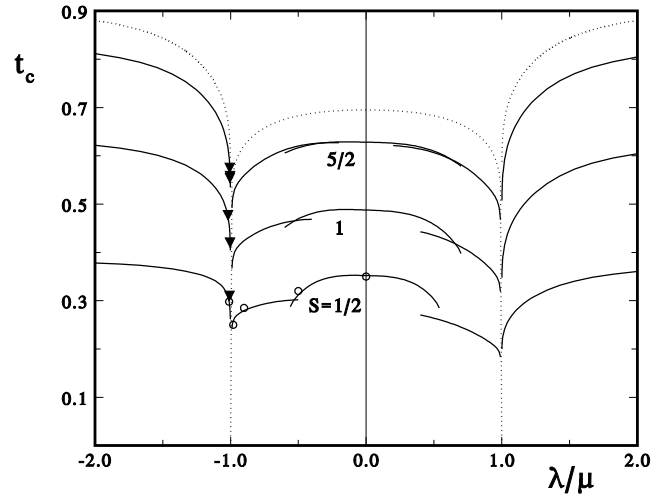


**Fig. 11.** Critical temperature *vs*  $\lambda/\mu$  for the class of models described by Eq. 1, with  $S = 1/2, 1, 5/2$ , and  $\infty$ ; symbols and curves as in Figs.8 and 9.

pletely agrees with that proposed by Ding in Ref. [29] on the basis of quantum MC data. In the antiferromagnetic  $S = 1/2$  easy-axis case, on the other hand, Branco and De Sousa [31] predict, from a real space renormalization group analysis, the existence of a critical  $\mu_c(1/2) \simeq -0.8$  at which  $t_I$  should vanish, and detect a reentrance in the  $\mu$  dependence of such temperature; they found no such anomaly in the ferromagnetic sector. This scenario is in contrast not only with ours and Ding's results, but also with experimental data.

Finally, from the experimental point of view, our results show that anisotropies, even if as small as those measured in most real compounds, are fundamental ingredients in determining the low-temperature behaviour of the materials; it is hence essential, in order to perform a meaningful analysis of the experimental data, to have at least an estimate of the temperature at which a possible BKT or Ising-like phase transition should occur. Our approach allows a determination of such temperature for any given value of  $S$  and  $\nu$ , therefore representing an important tool in the experimental investigation of two-dimensional Heisenberg magnets.

## 7 Acknowledgements

The authors wish to thank Dr. Luca Capriotti for his contribution in the early stage of the work. This research has been partially supported by the COFIN98-MURST fund.

## References

1. N. D. Mermin and H. Wagner, Phys. Rev. Lett. **17**, 1133 (1966).
2. E. Manousakis, Rev. Mod. Phys. **63**, 1 (1991).

3. V. L. Berezinskii, Zh. Eksp. Teor. Fiz **59**, 907 (1970).
4. J. M. Kosterlitz and D. J. Thouless, J. Phys. Condens. Matter **6**, 1181 (1973).
5. L. Onsager, Phys. Rev. *65*, 117 (1944).
6. See, e.g., A. F. M. Arts and H. W. de Wijn, in *Magnetic Properties of Layered Transition Metal Compounds*, ed. L. J. de Jongh, Kluwer Academic Publishers, Dordrecht (1990), pag. 191; J. Kanamori, in *Magnetism*, vol.1, ed. G.T. Rado and H. Suhl, Academic Press, New York (1963), pag. 127.
7. A. Cuccoli, V. Tognetti, P. Verrucchi and R. Vaia, Phys. Rev. A **45**, 8418 (1992).
8. A. Cuccoli, V. Tognetti, P. Verrucchi, and R. Vaia, Phys. Rev. B **46**, 11601 (1992).
9. A. Cuccoli, V. Tognetti, P. Verrucchi, and R. Vaia, Phys. Rev. B **56**, 14456 (1997).
10. A. Cuccoli, R. Giachetti, V. Tognetti, R. Vaia, and P. Verrucchi, J. Phys.: Condens. Matter **7**, 7891 (1995).
11. H. Weyl in *The theory of groups and quantum mechanics*, Dover, New York (1950).
12. J. Villain, J. Phys. (Paris) **35**, 27 (1974).
13. F. Holstein and H. Primakoff, Phys. Rev. **58**, 1048 (1940).
14. F.J. Dyson, Phys. Rev. **102**, 1217, (1956); S.V. Maleev, Zh. Eksp. Teor. Fiz. **33**, 1010 (1957).
15. A. Cuccoli, V. Tognetti, P. Verrucchi, and R. Vaia, Phys. Rev. B **51**, 12840 (1995).
16. L. Capriotti, A. Cuccoli, V. Tognetti, R. Vaia, and P. Verrucchi, Physica D **119**, 68 (1998).
17. A. Cuccoli, V. Tognetti, and R. Vaia, Phys. Rev. B **52**, 10221 (1995).
18. A. Cuccoli, T. Roscilde, V. Tognetti, P. Verrucchi, and R. Vaia, Phys. Rev. B **62**, 3771 (2000).
19. P. A. Serena, N. García, and A. Levanyuk, Phys. Rev. B **47**, 5027 (1993).
20. M. E. Gouvêa, G. M. Wysin, S. A. Leonel, A. S. T. Pires, T. Kampeter, and F. G. Mertens, Phys. Rev. B **59**, 6229 (1999).
21. H.-Q. Ding and M. S. Makivić, Phys. Rev. B **42**, 6827 (1990); Phys. Rev. B **45**, 491 (1992).
22. H.-Q. Ding, Phys. Rev. Lett. **68**, (1992); Phys. Rev. B **45**, 230 (1992).
23. H. W. de Wijn, L. R. Walker, and R. E. Walstedt, Phys. Rev. B **8**, 285, (1973).
24. J. Skalyo, Jr., G. Shirane, R. J. Birgeneau, and H. J. Guggenheim, Phys. Rev. Lett. **23**, 1394 (1969).
25. K. Nagata and Y. Tomono, J. Phys. Soc. Japan **36**, 78 (1974).
26. R. J. Birgeneau, H. J. Guggenheim, and G. Shirane, Phys. Rev. B **8**, 304 (1973).
27. B. Schröder, V. Wagner, N. Lehner, K.A.M. Kesharwani, and R. Geick, Phys. Stat. Sol. (b) **97**, 501 (1980).
28. R. A. Cowley, G. Shirane, R. J. Birgeneau, and H. J. Guggenheim, Phys. Rev. B **15**, 4292 (1977).
29. H.-Q. Ding, J. Phys.: Condens. Matter **2**, 7979 (1990).
30. J. Rossat-Mignod, L. P. Regnault, C. Vettier, P. Burlet, J.Y. Henry, and G. Lapertot, Physica B **169**, 58 (1991).
31. N. S. Branco and J. Ricardo de Sousa, preprint, cond-mat/0006345 (2000).